AIP | The Journal of Chemical Physics

Equilibrium Composition of Selenium Vapor; the Thermodynamics of the Vaporization of HgSe, CdSe, and SrSe

J. Berkowitz and W. A. Chupka

Citation: J. Chem. Phys. **45**, 4289 (1966); doi: 10.1063/1.1727488
View online: http://dx.doi.org/10.1063/1.1727488
View Table of Contents: http://jcp.aip.org/resource/1/JCPSA6/v45/i11
Published by the American Institute of Physics.

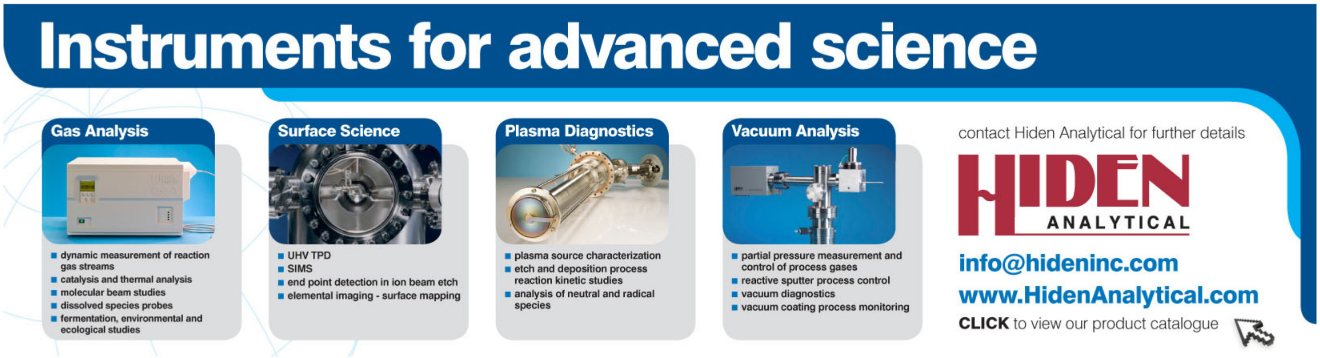

THE JOURNAL OF CHEMICAL PHYSICS VOLUME 45, NUMBER 11 1 DECEMBER 1966

Equilibrium Composition of Selenium Vapor; the Thermodynamics of the Vaporization of HgSe, CdSe, and SrSe*

J. BERKOWITZ† AND W. A. CHUPKA
Argonne National Laboratory, Argonne, Illinois

(Received 6 April 1966)

The vapor compositions of SrSe, CdSe, HgSe, hexagonal selenium, α-monoclinic selenium, and some mixed sulfur–selenium crystals have been studied by mass-spectrometric analysis. Dissociation energies of Se_2 (71.2±2 kcal/mole) and SrSe (59.1±3 kcal/mole) were obtained. The heats and free energies of formation of the various Se_n molecular species detected in the vapor are also given. There is no significant difference between the vaporization behavior of the two Se allotropes. Mixed sulfur–selenium molecules form very slowly at room temperature, but they form more readily at higher temperature, and quenching to room temperature retains the mixed configurations.

I. INTRODUCTION

THE experiments on selenium vapor to be described below had both remote and immediate stimuli from the sulfur vapor investigations[1] performed earlier in this laboratory. The immediate incentive arose while experiments were in progress to help answer the question: Do mixed rings of sulfur–selenium exist in substantial quantities in the vapor above a sulfur–selenium solution? This question had been pondered long ago by Muthmann[2] and rather recently had been revived by other workers.[3] In order to better understand such a problem, it became necessary to try to unravel the thermodynamic factors from the kinetic factors, and this naturally led to an investigation of the thermodynamic properties of selenium rings in comparison with sulfur rings. The remote interest stemmed in part from a desire to see whether the nonequilibrium behavior noted in the vaporization of certain sulfur allotropes would manifest itself also in the vaporization of different selenium crystal structures. Along these lines, it may be recalled that three interesting sulfur allotropes were previously studied.[1]

(1) The stable, crystalline orthorhombic sulfur, which can be described as a molecular lattice, each lattice point being a puckered S_8 ring. Evaporation from a single-crystal face of such a lattice yielded practically only S_8 molecules.

(2) The long-lived metastable S_μ, a long-chain polymer of sulfur, which vaporized to give S_8, S_7, and S_6 molecules.

(3) A metastable crystalline structure called "Engel's sulfur" or S_ρ, whose behavior is analogous to that of (1) above. The molecular lattice consists of S_6 units, and the vapor is predominantly S_6 upon direct vaporization.

The analogs to Forms (1) and (2) exist in selenium, although there is a reversal in stability. That allotrope which is the stable crystalline form of selenium at room temperature and up to 217°C is called hexagonal selenium or metallic selenium and has essentially the long-chain form. The metastable species is termed α-monoclinic selenium and may be thought of as Se_8 rings[4] held together by van der Waals forces. There also exists an allotrope referred to in the literature as β-selenium[5,6] whose structure is evidently very similar to that of α-selenium.[6] No analog to the six-membered-ring structure [Type (3) above] has been found for selenium.

Hence, both free-evaporation studies and Knudsen-cell experiments were undertaken with the selenium allotropes in order to test for the presence of nonequilibrium vaporization. Both types of investigations employed mass-spectrometric techniques that had been successfully developed for the study of sulfur vapor. Thus, the partial pressures of various selenium molecules produced by the dissociative vaporization of HgSe, CdSe, and SrSe could be used to infer the various equilibria existing among these species. This information could then be utilized to calculate the composition of the saturated vapor of selenium. (Direct measurement of this composition by mass-spectrometric techniques is thwarted by the excessive fragmentation that ensues upon electron impact.)

Initial experiments showed that the mass spectrum

---

* Work performed under the auspices of the U.S. Atomic Energy Commission.

† Currently at the Physikalisches Institut der Universität, Freiburg, West Germany on a Guggenheim Foundation Fellowship.

[1] (a) J. Berkowitz and J. R. Marquart, J. Chem. Phys. 39, 275 (1963); (b) J. Berkowitz and W. A. Chupka, *ibid.* 40, 287 (1964); (c) J. R. Marquart and J. Berkowitz, *ibid.* 39, 283 (1963); (d) J. Berkowitz, in *Elemental Sulfur*, B. Meyer, Ed. (John Wiley & Sons, Inc., New York, 1965), Chap. 7.

[2] W. Muthmann, Z. Krist. 17, 336 (1890).

[3] (a) L. M. Lapina and V. V. Illarionov, Zh. Neorg. Khim. 3, 1210 (1958); (b) L. M. Lapina, *ibid.* 3, 1386 (1958); (c) A. I. Soklakov and V. V. Illarionov, J. Inorg. Nucl. Chem. 6, 647 (1961); (d) Y. de Haan and M. Visser, Physica 26, 127 (1960).

[4] R. D. Burbank, Acta Cryst. 4, 140 (1951).

[5] R. D. Burbank, Acta Cryst. 5, 236 (1952).

[6] R. E. Marsh, L. Pauling, and J. D. McCullough, Acta Cryst. 6, 71 (1953).

resulting from HgSe was not sufficiently different from that of ordinary selenium to provide information regarding fragmentation effects, and the CdSe vaporization produced barely detectable amounts of Se_3. Hence the intermediate-temperature region, for which the vapor in the sulfur experiments was so conveniently provided by (especially) HgS, was absent in the selenium case. In order to fill in this significant temperature–pressure region, a variant of the double-oven approach was employed, as is described in the experimental section.

In the course of this investigation, the dissociation energy of Se_2 was also determined, largely from the results of the experiments on evaporation of SrSe. In order to rule out the uncertainty regarding ionization cross sections, the relative values of this quantity for Sr, Se, Se_2, Cd, and Ag were determined in separate experiments.

Another point of some interest is the comparison of the current results with the measurements of the average molecular weight of selenium vapor. Several such measurements exist,[7] and the comparison serves as a crude check on the detailed equilibrium constants obtained from the mass-spectrometric results and their variation with temperature, which in turn provides information regarding the energies of transformation among the various Se_n molecular species.

II. EXPERIMENTAL ARRANGEMENT

A. Oven Assemblies

Much of the experimental technique and equipment was identical to that employed in the equilibrium[1a] and nonequilibrium[1b] studies of sulfur vapor. One of the innovations required by this particular experiment was the use of one oven within another. A platinum tube of ~5-mm diameter, was closed at one end and filled with sample [either the metallic-grey selenium (distilled) or HgSe]. Then the other end was crimped around a wire of known diameter to provide the "first" effusion hole. This entire assembly was placed within a molybdenum oven having an effusion hole of larger area. In one typical experiment, the first effusion hole had a 0.006-in. diameter, the second was of 0.040-in. diameter. The ratio of areas was quite critical because the relative concentration of Se_6 and Se_2, for example, varies rapidly with pressure at a given temperature.

The ovens used for equilibrium experiments were of molybdenum; for surface evaporation, platinum boats were employed. In the former case, the temperature was measured with a Pt/Pt–10% Rh thermocouple except in the SrSe experiment, in which a W/W–26% Rh thermocouple was used with the calibration supplied by the manufacturer.

B. Preparation of Sample

1. Hexagonal Selenium

Commercial-grade selenium powder was distilled in vacuum. Only the middle portion was retained.

2. α-Selenium

The purified selenium was heated above the melting point, quenched in cold water and allowed to dry. The resulting solid was ground to a fine powder and the α-selenium extracted with carbon disulfide. Small crystals (~0.2 mm on an edge) were obtained by slowly evaporating the saturated (orange) solution.

3. Mixed Sulfur–Selenium Crystals

Four different samples were prepared as follows. (1) The CS_2 solution saturated in α-selenium (above) was also saturated with pure orthorhombic sulfur crystals. The resulting solution was allowed to evaporate slowly. The crystals obtained were large and distinctly more orange than orthorhombic sulfur crystals, but the selenium content deduced by chemical analysis was only ~0.1%. (2) A mixed crystal from Preparation (1) above (~0.1% Se) was dissolved in a saturated solution of α-monoclinic selenium in CS_2. The precipitation was permitted to take place slowly over a three-week period. After decanting the excess CS_2, small crystals ($\lesssim$1 mm on an edge) were removed. They appeared to turn black in air, but under a microscope they appeared red by transmitted light. (3) A mixture of 30% Se/70% S (by weight) was heated to 300°C in a sealed evacuated tube and maintained at that temperature for 2–3 h, then permitted to cool very slowly past the freezing point. The resulting solid was crushed, and several well-formed crystals were selected for mass analysis. (4) Some crystals from Preparation (3) above were dissolved in CS_2 and then permitted to recrystallize from this solution over a two-month period. At this time, a beautiful needlelike crystal, 10–15 mm long and having a ruby-red color, was removed and loaded into the sample holder.

4. HgSe

Stoichiometric amounts of Hg and hexagonal selenium powder were heated in a sealed evacuated tube to 300°C for ~2 h, then permitted to cool slowly.

5. SrSe

This compound was prepared by the reduction of $SrSeO_3$ with ammonia at about 850°C. The $SrSeO_3$

---

[7] (a) G. Preuner and I. Brockmöller, Z. Physik. Chem. **81**, 129 (1912); (b) K. Neumann and E. Lichtenberg, *ibid.* **184**, 89 (1939); (c) K. Niwa and Z. Shibata, J. Fac. Sci. Hokkaido Imp. Univ. **3**, 52 (1940); (d) V. V. Illarionov and L. M. Lapina, Dokl. Akad. Nauk SSSR **114**, 1021 (1957) [English transl.: Soviet Phys.–Doklady **114**, 615 (1957)].

was formed from the previously distilled selenium by use of a standard procedure.[8]

6. CdSe

Ultrahigh-purity material, obtained from Electronic Space Products, Inc., was used.

III. EXPERIMENTAL RESULTS

The discussion of the composition of the selenium vapor parallels that for sulfur.[1a] The simplest species, produced at the highest temperatures, is examined first, and the degree of complexity is gradually increased so that one may better appreciate the emergence of a new species or the influence of fragmentation. At the lowest temperatures, the different allotropes of selenium and the mixed crystals are investigated by mass analysis of their respective vapors produced by surface evaporation.

TABLE I. Mass spectrum of strontium selenide at $T=1852._8$°K. The energy of the ionizing electrons was 75 eV. The peak intensities shown have already been corrected for the secondary-electron yield at the multiplier.

Vapor species	Peak intensity (arbitrary units)
^{80}Se	660
^{88}Sr	1110
^{160}(Se$_2$)	5.0_4
^{168}(SrSe)	8.7

A. Strontium Selenide

A typical mass spectrum of SrSe vapor is shown in Table I. The sample vaporized congruently to completion. This property of SrSe, together with its simple mass spectrum, made it very convenient to perform pressure calibrations. Known weights of the sample could be evaporated to completion, the oven temperature being maintained constant. The Sr^+ and Se^+ peaks were alternately monitored in these experiments. In this way, separate pressure calibrations could be performed on Sr and Se, and their relative ionization cross sections could be directly determined. In some experiments a weighed amount of silver was also introduced and evaporated to completion, thus providing relative ionization cross sections for Sr, Se, and Ag. These values, corrected for the molecular velocities through the ionization chamber, are shown in Table II. An average of several pressure calibrations for Sr and Se at 1853°K yielded for each the partial pressure $1.2\pm0.3\times10^{-5}$ atm. No accurate measurement of the temperature dependence of these species was attempted.

TABLE II. Relative ionization cross sections by electron impact. The energy of the ionizing electrons was 75 eV. All cross sections are expressed as ratios to that for Ag.

Vapor species	Ionization cross section
Se	$1.5_0\pm0.2_5$
Se$_2$	0.88 ± 0.05
Sr	$1.3_3\pm0.2_5$
Cd	$0.7_0\pm0.1_0$

B. Cadmium Selenide

This vaporization does not proceed congruently. Initially cadmium volatilizes much more rapidly. Then, for about half the vaporization, the ratios of Cd^+ and Se_2^+ remain constant. About midway through the evaporation, there appears to be a rather sudden discontinuity at which the Se_2^+ rises and the Cd^+ falls by about a factor of 2. A typical mass spectrum characteristic of the stable period after the initial loss of Cd is shown in Table III. The temperature shown there is relatively high because Se_3^+ could be detected only at the highest temperatures. Although the evaporation of CdSe was not as convenient as that of SrSe, a similar scheme was used to evaluate partial pressures and relative ionization cross sections, including that of Ag, by evaporation to completion. Table II includes these relative ionization cross sections. On comparing with the SrSe data, one notes the surprising result that the cross section of atomic Se is larger than that of diatomic selenium. Figure 1 locates several points on a plot of $\log P$ vs $1/T$, where $P=P(\text{Cd})+P(\text{Se}_2)$. Since CdSe does not vaporize without change of composition, this method of displaying the data does not have fundamental significance, but it is useful for comparing the present data with the results of previous workers, who implicitly assumed stoichiometric vaporization. Also shown in Fig. 1 are the data of Pashinkin[9] who used Knudsen effusion, Somorjai[10] who used

TABLE III. Mass spectrum of cadmium selenide at $T=971._0$°K. The energy of the ionizing electrons was 75 eV. The peak intensities shown have already been corrected for the secondary-electron yield at the multiplier.

Vapor species	Peak intensity (arbitrary units)
^{80}Se	80 640
^{114}Cd	609 000
^{160}(Se$_2$)	360 000
Se$_3$	67.5
Se$_4$	$\leqslant 3.0$

---

[8] G. Brauer, *Handbook of Preparative Inorganic Chemistry* (Academic Press Inc., New York, 1963), 2nd ed., Vol. 1.

[9] A. S. Pashinkin, J. Inorg. Nucl. Chem. **7**, 1367 (1962).

[10] G. A. Somorjai, J. Phys. Chem. **65**, 1059 (1961).

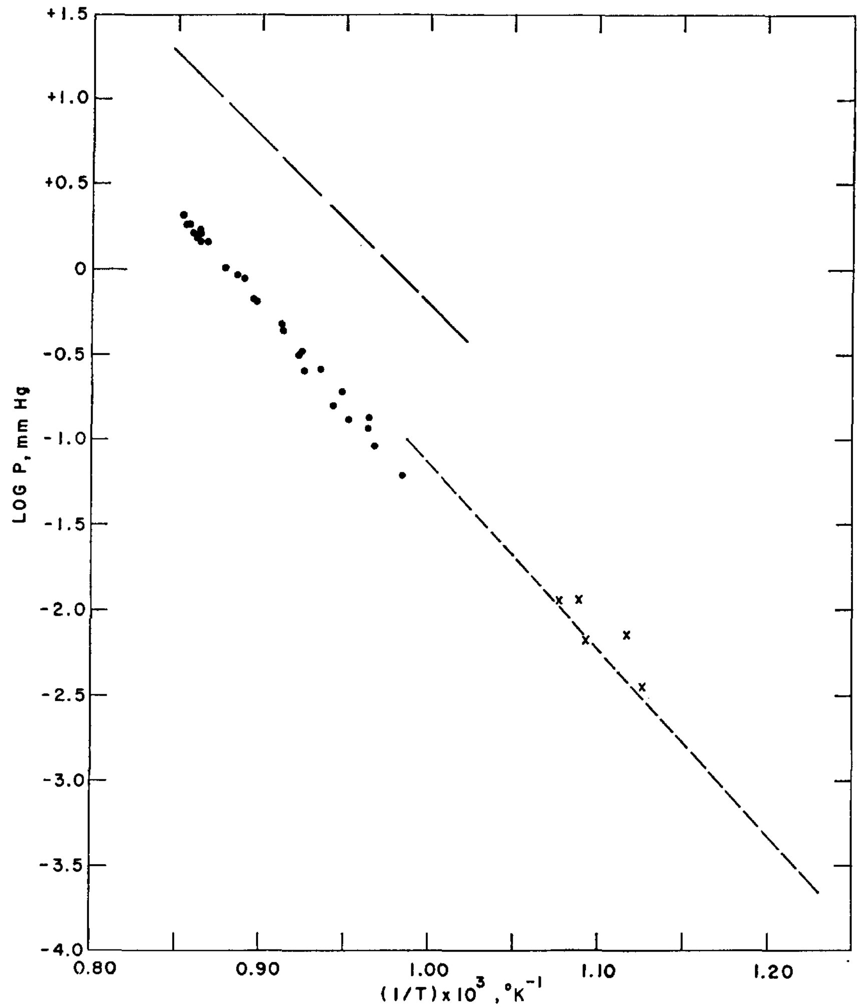

FIG. 1. Semilogarithmic plot of the total vapor pressure of CdSe ($Cd+\frac{1}{2}Se_2$): (a) —— Somorjai, Ref. 10; (b) ---- Pashinkin, Ref. 9; (c) ●, Wösten, Ref. 11; (d) ×, present data. Only the present data take nonstoichiometric vaporization into account.

Bourdon-gauge and dew-point methods, and Wösten[11] who used a transpiration technique. It is readily seen that the present data are in good agreement with those obtained by the Knudsen-effusion and transpiration techniques, but the data of Somorjai are too high by a factor of 10. The experimental points in the current study that deviate farthest from Pashinkin's data correspond to the largest departure from stoichiometric vaporization. An earlier mass-spectrometric study[12] also concluded that Somorjai's vapor pressure data were questionable. However, the unexpected value of the ratio of ionization cross sections for Se_2^+ and Se^+ was not found by these authors. Their method for arriving at this ratio was less direct since it involved the use of calculated atomic ionization cross sections. Extensive measurements of the temperature dependence of this vapor pressure were not undertaken in this study.

C. Mercuric Selenide

The mass spectrum of this sample did not remain constant during the evaporation. This could be due to incomplete reaction of the Hg and Se reactants in the preparation, a slight excess of one of the reactants above the stoichiometric limit, or to nonstoichiometric vaporization of the stoichiometric compound.[13] A typical mass spectrum in the middle of a vaporization run is seen in Column 1 of Table IV. Goldfinger and Jeunehomme[12] also tabulate a mass spectrum for HgSe. Direct comparison is not meaningful, since the degree of departure from stoichiometric vaporization is the principal determinant of the discrepancy. Nevertheless, there remain large differences which cannot be explained in this way. We observe the Se_5^+ more intense than Se_6^+ by a factor 1.8, whereas Goldfinger and Jeunehomme[12] observe Se_6^+ greater than Se_5^+ by a factor 6.4. Also, the latter authors attempt to draw some conclusions regarding the free energy of formation of HgSe from the Se_2^+ ion intensity, whereas our analysis (see Sec. F, below) leads to the conclusion that the Se_2^+ observed by these authors must be predominantly from fragmentation of Se_6.

---

[11] W. J. Wösten, J. Phys. Chem. 65, 1949 (1961).

[12] P. Goldfinger and M. Jeunehomme, Trans. Faraday Soc. 59, 2851 (1963).

[13] After completion of this manuscript, the article of R. F. Brebrick, J. Chem. Phys. 43, 3846 (1965) appeared, and helps explain the shifting vapor composition. From his observations, it is clear that the stoichiometric range is very narrow (less than 1 at. %) and complete reaction of Hg and Se requires a temperature of at least 630°C.

D. Hexagonal Selenium

The mass spectrum of the vapor of this sample effusing from a Knudsen cell is shown in Column 2 of Table IV. The most significant difference between Columns 1 and 2 is seen for Se_6^+, Se_7^+, and Se_8^+. This is just the region in which either sample by itself gives sufficient information since the rapid decline in ion intensity from Se_6^+ toward Se_8^+ enables one to argue on plausibility grounds that fragmentation effects will not substantially alter the ratio of parent-ion intensities. This is in marked contrast to the situation in sulfur. There, the mass spectrum of equilibrium vapor above pure sulfur had its maximum at the S_8^+ ion position, and hence all lower mass peaks could receive substantial contributions from fragmentation. The use of HgS as a source of sulfur vapor clearly shifted the equilibrium to a condition for which S_6^+ was most intense. In the present case of selenium, the use of HgSe has likewise shifted the spectrum somewhat, so that Se_5^+ replaces Se_6^+ as the most abundant species in this mass range; but HgSe is not nearly as useful as HgS was in the sulfur investigation.

TABLE IV. Mass spectra of mercuric selenide and hexagonal selenium (from a Knudsen cell) and of α-selenium and hexagonal selenium by surface evaporation. In each case, the ion-multiplier intensity of the most abundant isotope has been taken without correcting for the secondary-electron yield. The energy of the ionizing electrons is 75 eV in each instance.

Vapor species	HgSe Knudsen cell $T=566°K$	Hexagonal Se		α-Se
		Knudsen cell $T=544°K$	Surface evaporation	Surface evaporation
Se^+	∼40	34.9	...	58.1
Se_2^+	100.0	100.0	100.0	100.0
Se_3^+	25.2	31.2	32.8	37.2
Se_4^+	10.0	16.4	28.6	37.2
Se_5^+	34.2	31.7	48.6	38.3
Se_6^+	19.3	36.3	84.3	93.0
Se_7^+	3.3	11.5	19.3	18.6
Se_8^+	0.3	1.9	2.9	2.8
Se_9^+				0.01
Hg^+	226.0			

E. Measurements of the Temperature Dependence

The preceding survey of mass spectra provides sufficient information to enable us to draw some plausible conclusions regarding the composition of the vapor under various conditions, and hence to adjust the succeeding experiments accordingly. For example, the equilibrium involving Se_6 and Se_8 can be studied as a function of temperature with either the hexagonal selenium or HgSe sample. A graph of log$K$ vs $1/T$ for the reaction

$$3Se_8 \rightarrow 4Se_6 \tag{1}$$

is shown in Fig. 2. The slope of the best straight line yields +16.5 kcal/mole for the enthalpy change of this reaction. A corresponding plot for the reaction

$$6Se_7 \rightarrow 7Se_6 \tag{2}$$

is shown in Fig. 3. The slope of this curve yields +14.1 kcal/mole for the enthalpy change of Reaction (2).

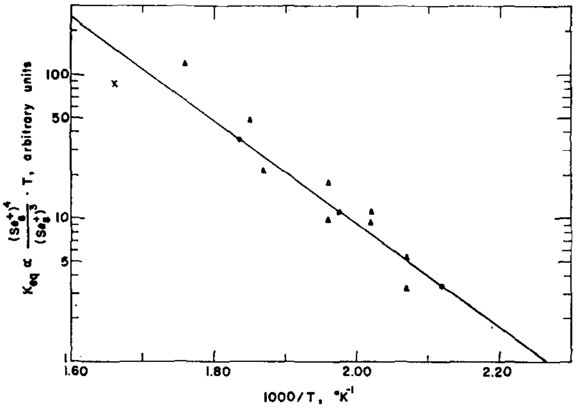

FIG. 2. Semilogarithmic graph of K vs $1/T$ for the equilibrium $3Se_8(g) \rightarrow 4Se_6(g)$, where each partial pressure is proportional to the corresponding ion intensity and the absolute temperature. ●, pure selenium; △, HgSe; and ×, double oven. The line is drawn through the data for pure selenium.

Beyond this point, one must exercise caution. The vapor above selenium cannot be relied upon as a good measure of the Se_6–Se_5 equilibrium since $I(Se_6^+) > I(Se_5^+)$. This situation is reversed in the vapor above HgSe, and hence the equilibrium

$$5Se_6 \leftrightarrow 6Se_5 \tag{3}$$

could be studied with this system. However, a more unambiguous condition was attained with the double-

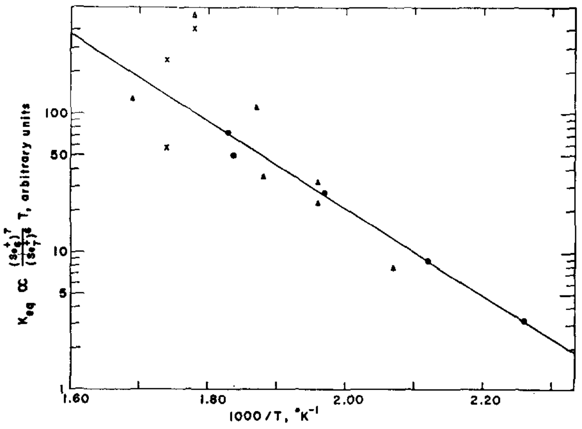

FIG. 3. Semilogarithmic graph of K vs $1/T$ for the equilibrium $6Se_7(g) \rightarrow 7Se_6(g)$, where each partial pressure is proportional to the corresponding ion intensity and the absolute temperature. ●, pure selenium; △, HgSe; and ×, double oven. The line is drawn through the data for pure selenium.

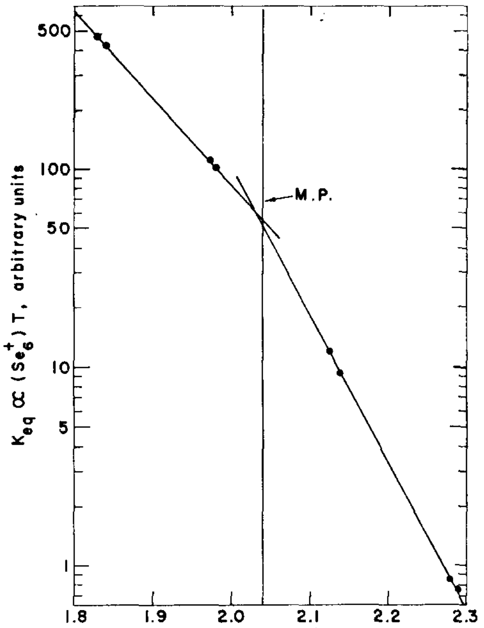

FIG. 4. Semilogarithmic graph of K vs $1/T$ for the equilibrium 6Se (condensed)→Se_6(g).

oven arrangement, and hence further study of the equilibrium given by Eq. (3) is described below. Any further attempt to relate the molecular species with the aid of the systems described above is subject to the strong probability of confusion because of fragmentation.

Before proceeding to more delicate measurements, one further experiment should be mentioned. If one defines the heat of fusion of selenium as the enthalpy change of the reaction

$$\mathrm{Se(solid)} \rightarrow \mathrm{Se(liquid)}, \qquad (4)$$

then one should be able to arrive at an experimental value for this quantity by summing any one set of the reactions

$$\mathrm{Se(s)} \rightarrow n^{-1}\,\mathrm{Se}_n\mathrm{(g)},$$

$$n^{-1}\,\mathrm{Se}_n\mathrm{(g)} \rightarrow \mathrm{Se(l)}. \qquad (5)$$

In this case, the difference between the heat of sublimation and heat of vaporization of any of the species Se_6, Se_7, or Se_8 can serve as a measure of the heat of fusion, via Eqs. (5) above. The nature of the relations in Eqs. (5) permits of relatively high accuracy in the determination of the heat of fusion, as can be seen in Fig. 4 where measurements on Se_6 have been chosen for the calculation. The measured intensities of Se_6^+ have been chosen for the calculation because of their larger values and consequent higher accuracy. The resulting value of 2.3_0 kcal/mole for the heat of fusion corresponding to Reaction (4) differs from the accepted[14] value of 1.3 kcal/mole by more than the present experimental error.

F. Double-Oven Experiments

The thermodynamic data described above enable us to relate the stability of Se_8 and Se_7 to that of Se_6, and the latter in turn to the condensed phase. We also have a relation between monatomic Se and Se_2, and some information on Se_3. In order to tie these two groups of data together (and hopefully to obtain information on the missing species), it would be desirable to find a temperature–pressure region in which, for example, Se_6 and Se_2 could be clearly identified as parent ions. This implies a pressure such that Se_6^+ is substantially less intense than Se_2^+ in order to minimize fragmentation effects. Since it was not obvious that the equilibrium vapor above HgSe (Column 1 of Table IV) satisfied these requirements, we decided upon a trial-and-error approach with the double-oven arrangement described in Sec. II.A. The orifice of the inner oven was adjusted from one experiment to the next until the conditions $Se_6^+ < Se_2^+$ was satisfied and in addition the Se_6^+ was measurable over a substantial temperature range. The graph of log$K$ vs $1/T$ (Fig. 5) for the reaction

$$Se_6 \rightarrow 3Se_2 \qquad (6)$$

was obtained in this way by use of an inner oven having

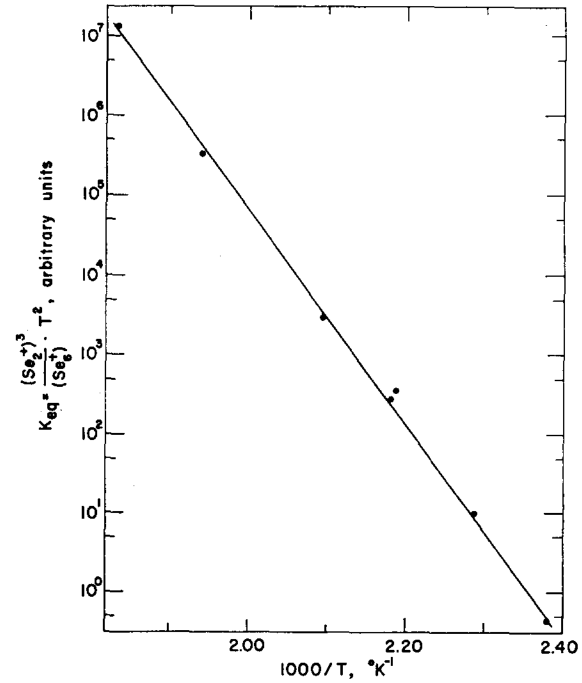

FIG. 5. Semilogarithmic graph of K vs $1/T$ for equilibrium Se_6(g)→$3Se_2$(g), where each partial pressure is proportional to the corresponding ion intensity and the absolute temperature.

---

[14] R. D. Stull and G. C. Sinke, Advan. Chem. Ser. **18**, 179 (1956).

an orifice 0.005 in. in diameter. The best straight line through the experimental points has a slope equivalent to +61.7 kcal/mole for Reaction (6). However, it is seen later in the discussion of surface evaporation that even in this optimum condition there were still contributions from fragmentation. To a good approximation, the ratio of fragment ion to parent ion is constant over a short temperature range. From this observation, one can infer that the influence of fragmentation will be most apparent when the ratio $I(Se_6^+)/I(Se_2^+)$ is highest, i.e., at the lower temperatures in Fig. 5. Subtracting fragmentation effects will therefore result in an increased slope for this plot. Detailed considerations of the extent of fragmentation, weighting the upper temperature points most heavily, lead to a corrected value of 65 kcal/mole for the enthalpy change in Reaction (6) at ~550°K.

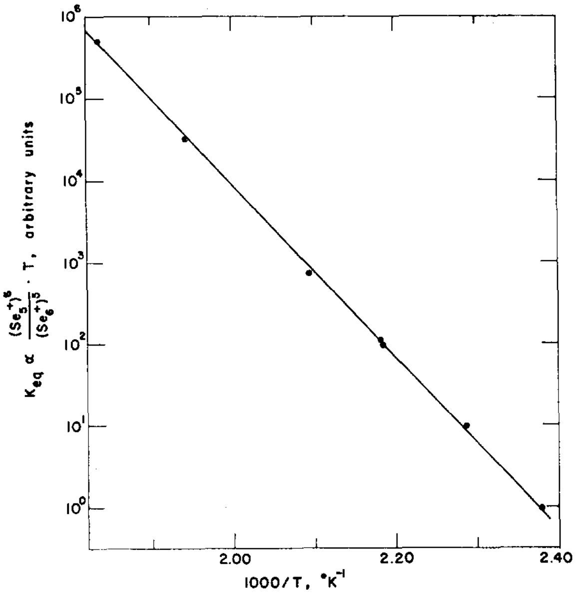

FIG. 6. Semilogarithmic graph of K vs $1/T$ for the equilibrium $5Se_6(g) \rightarrow 6Se_5(g)$, where each partial pressure is proportional to the corresponding ion intensity and the absolute temperature.

The same conditions that optimize the Se_6:Se_2 equilibrium proved ideal for studying the Se_6:Se_5 behavior. The temperature dependence of Reaction (3), shown in Fig. 6, results in an enthalpy change of +55.2 kcal/mole for that reaction.

In order to investigate the Se_2:Se_3 equilibrium over an extended temperature range, one further nuance was added. Instead of placing selenium in the inner oven, HgSe was used as the "feed." This particular sample had been previously evaporated for some time so that the partial pressure of selenium species was reduced. The inner oven had an orifice of 0.010-in. diameter for optimum conditions. In addition to this sample, the outer oven contained some CdSe. In this way, it was hoped that the Se_2:Se_3 equilibrium could be studied in the lower temperature range by using the HgSe as a source of vapor. Then, when this sample was exhausted, the upper temperature range could be examined by use of the CdSe source without changing the geometric properties or the sensitivity of the apparatus. The results of this experiment for the reaction

$$2Se_3 \rightarrow 3Se_2, \qquad (7)$$

expressed in the usual log$K$-vs-$1/T$ form, are seen in Fig. 7. The slope is equivalent to an enthalpy change of $+25.7_6$ kcal/mole.

TABLE V. Experimental enthalpy changes for the various selenium species, as obtained by measurements of the temperature dependence.

Reaction	Temperature, T (°K)	Enthalpy change, ΔH_T (kcal/mole)
$2Se_3 \rightarrow 3Se_2$	850	$+25.7_6$
$Se_6 \rightarrow 3Se_2$	475	$+65$
$5Se_6 \rightarrow 6Se_5$	500	$+55.2$
$6Se_7 \rightarrow 7Se_6$	500	$+14.1_4$
$3Se_8 \rightarrow 4Se_6$	500	$+16.5$
6Se (solid) $\rightarrow Se_6$	460	$+33.7_7$
6Se (liquid) $\rightarrow Se_6$	525	$+19.9_4$

All of the results of the temperature-dependence measurements are summarized in Table V. It is noted that virtually no information is available for Se_4, the best being a limit noted in Table III. The situation is only slightly better with S_4^+, which is definitely observed as a parent in the ZnS and CdS experiments but for which no reliable temperature dependence has been obtained.[1d]

G. Surface-Evaporation Experiments

The mass spectra obtained from α-selenium and hexagonal selenium, each evaporating from a surface

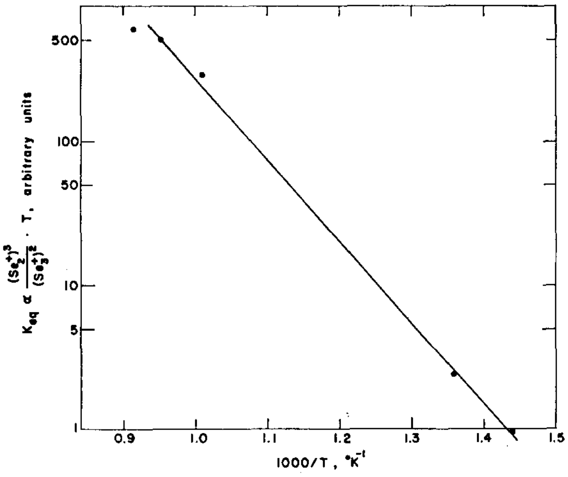

FIG. 7. Semilogarithmic graph of K vs $1/T$ for the equilibrium $2Se_3(g) \rightarrow 3Se_2(g)$, where each partial pressure is proportional to the corresponding ion intensity and the absolute temperature.

rather than in a "hohlraum," is shown in Columns 3 and 4 of Table IV. Some temperature dependence was observable for these spectra; the data for α-selenium correspond to a relatively low temperature which was necessary to minimize conversion to the stable allotrope. The differences in the two surface-evaporation spectra are rather small, in marked contrast to the corresponding results in sulfur in which orthorhombic sulfur and S_μ had very different mass spectra. One is drawn to the conclusion that the two spectra are similar enough to be due to the same antecedent. In other words, it is plausible to infer that the rate of conversion of α-selenium to hexagonal selenium is so fast at the temperature of the experiment that one cannot measure the surface evaporation of α-selenium itself.

There does appear to be a significant difference between either of the surface-evaporation experiments and the Knudsen-cell result (Column 2 of Table IV). Some of this difference may be attributable to the method of normalizing, choosing $Se_2^+=100$, since part of the "shutter effect" of this peak has sometimes been found to be coming from extraneous sources. Nevertheless, the ratios $Se_6^+:Se_5^+$ in Column 2 are different enough from those in Columns 3 and 4 to suggest that Se_6 is a favored species in the free evaporation of selenium.

It is shown later by thermodynamic arguments that Se_2 is a minor component of the saturated vapor of selenium. Indeed, this can be inferred from some of the vapor-density experiments.[7] The optical absorption measurements of Brebrick[15] also draw this conclusion. Hence, the strong ion intensity at the Se_2^+ position is to be attributed largely to fragmentation. The previous studies enable one to conclude that most of this fragmentation is from Se_5 and Se_6. The sum of Se_5^+ and Se_6^+ in each of the columns 2, 3, and 4 of Table IV is very roughly the same as Se_2^+, and hence one can use this crude fragmentation pattern to correct the $Se_2:Se_6$ equilibrium shown in Fig. 5 by subtracting the $Se_6^++Se_5^+$ intensity from the observed Se_2^+ intensity. With this correction, the three highest temperature points are virtually unchanged.

H. Mixed-Crystal Experiments

The order in which the experiments are described below agrees with the order followed in preparing the sulfur–selenium samples (Sec. II.B). All of the mass spectra in this section were obtained by surface evaporation.

1. Crystal Prepared by Coprecipitation

The mass spectrum was substantially that of orthorhombic sulfur, with the additional presence of small amounts of S_7Se^+ and still smaller amounts of $S_6Se_2^+$. At ~350°K, a temperature such that the crystal had not yet melted, the abundance ratios were $S_8^+:S_7Se^+:S_6Se_2^+=7550:12.2:1.0$.

2. Crystal from Sec. 1 Dissolved in Saturated α-Selenium Solution and Reprecipitated

As might be expected, the crystals obtained in this instance produced a mass spectrum virtually identical to that of pure selenium. In this experiment, the sample was evaporated completely, and the final stages of evaporation were slow enough to permit several measurements of the various Se_n^+ peaks as the pressure diminished. Analysis of the resulting data has proved useful as a qualitative test of the relative importance of fragmentation and primary ionization as a contribution to the intensity of a particular Se_n^+.

For example, let us suppose that the Se_4^+ ion is predominantly a fragment of Se_6. Then the intensity ratio $I(Se_4^+)/I(Se_6^+)$ will remain constant as the sample pressure diminishes. Hence, a plot of

$$\log[I(Se_6^+)/I(Se_4^+)] \text{ vs } \log I(Se_6^+)$$

will have zero slope. Now let us make the contrary assumption that Se_4^+ is a parent ion and that Se_4 and Se_6 are always in equilibrium. Then

$$[I(Se_4)]^3/[I(Se_6)]^2=K=\text{const.} \tag{8}$$

Hence, by simple manipulation,

$$\log[I(Se_6^+)/I(Se_4^+)]=-\tfrac{1}{3}\log K+\tfrac{1}{3}\log I(Se_6^+).$$

A plot of $\log[I(Se_6^+)/I(Se_4^+)]$ vs $\log I(Se_6^+)$ will thus have a slope of $\frac{1}{3}$. If both fragmentation and primary ionization contribute significantly to Se_4^+, the slope should lie somewhere between 0 and $\frac{1}{3}$. Similar equations can be developed for the other equilibrium partners of Se_6, the resulting slopes for Se_2, Se_3, and Se_5 being $\frac{2}{3}$, $\frac{1}{2}$, and $\frac{1}{6}$, respectively.

Log–log plots of the experimental results for the various intensity ratios $I(Se_6^+)/I(Se_n^+)$ as a function of $I(Se_6^+)$ are shown in Fig. 8. It is readily seen that Se_4^+ behaves as a fragment of Se_6, the limiting slope being practically zero even as S_6 becomes very small. The slope for Se_2^+ is distinctly greater than zero, but less than the value $\frac{2}{3}$ expected if it were predominantly a parent ion. As we have already noticed in the earlier discussions, the apportioning of the ion intensity of Se_2 between fragmentation and primary ionization presents difficulties. For Se_5^+, the behavior in Fig. 8 seems to lend credence to the view that it is a parent ion, although the difference between the two alternatives in this case causes only a change of slope from zero to $\frac{1}{6}$. The Se_3^+ appears to behave predominantly as a fragment ion when the Se_6 has a high pressure; but at the lowest pressures a departure from zero slope is evident and may indicate the beginning of competition between parent ionization and fragmenta-

---

[15] R. F. Brebrick, J. Chem. Phys. **43**, 3031 (1965).

tion as contributors to Se_3^+. All of the semiquantitative conclusions drawn from Fig. 8 are in agreement with the arguments presented earlier. A graph similar to Fig. 8 could of course be constructed on the assumption that Se_5 is the parent, but the results of such a plot are still only semiquantitative and do not alter the conclusions.

3. *Crystals Prepared from Melt at* 300°C

The very rich mass spectrum that results upon analysis of the vapor from these crystals can be seen in Table VI. The table has been arranged in groupings corresponding to the total number of atoms in the molecular ion. It is noteworthy that within each group there is a stepwise loss of intensity by about a factor of 3–4 each time a sulfur is replaced with a selenium atom.

The simplest interpretation of this spectrum is as follows. (a) The equilibrium being measured most probably corresponds to that established at the high temperature (300°C). This equilibrium is then "frozen in" by permitting the sample to cool and crystallize. (b) At 300°C, the formation of pure sulfur, pure selenium, or mixed molecules seems approximately random. (c) The stepwise diminution in intensity upon substitution of Se for S is most probably due to the lowering of the volatility of the species. Thus, even though the initial melt contained only ~15 mole % Se, it is plausible that the reaction produced enough material of each species Se_mS_n to generate a partial pressure close to that corresponding to unit activity. In this last statement we implicitly are treating each Se_mS_n species as a separate component, which is legitimate if they do *not* interchange atoms at a rate that is rapid relative to the measurement time. On the basis of the conclusions reached in Secs. 1 and 2 above, this seems a reasonable assumption.

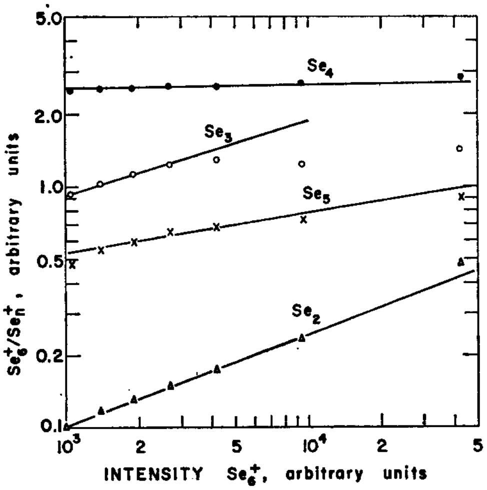

FIG. 8. Log–log graph of $[I(Se_6^+)/I(Se_n^+)]$ vs $I(Se_6^+)$ as the selenium sample evaporates to dryness.

TABLE VI. Mass spectrum from crystals obtained after freezing a 30% selenium–70% sulfur melt.[a]

Species	Intensity
S_8 group	
S_8^+	1600
S_7Se^+	620
$S_6Se_2^+$	160
$S_5Se_3^+$	32
$S_4Se_4^+$	6.0
$S_3Se_5^+$	1.5
S_7 group	
S_7^+	300
S_6Se^+	130
$S_5Se_2^+$	32
$S_4Se_3^+$	9.0
$S_3Se_4^+$	3.5
S_6 group	
S_6^+	730
S_5Se^+	370
$S_4Se_2^+$	160
$S_3Se_3^+$	43
$S_2Se_4^+$	13
SSe_5^+	4.0
Se_6^+	2.5
S_5 group	
S_5^+	1150
S_4Se^+	460
$S_3Se_2^+$	120
$S_2Se_3^+$	Hidden by S_7Se isotopes
SSe_4^+	Hidden by S_6Se_2 isotopes
Se_5^+	Hidden by S_5Se_3 isotopes
S_4 group	
S_4^+	1300
S_3Se^+	420
$S_2Se_2^+$	75
SSe_3^+	Hidden by S_6Se isotopes
Se_4^+	Hidden by S_5Se_2 isotopes
S_3 group	
S_3^+	630
S_2Se^+	190
SSe_2^+	40
Se_3^+	Hidden by S_5Se isotopes
S_2 group	
S_2^+	4260 (probably not all shutter)
SSe^+	575
Se_2^+	130

---

[a] This mass spectrum was obtained with 75-eV electrons. The intensities given are ion-multiplier values of the most abundant isotopic mass of each species, uncorrected for the secondary-electron yield at the multiplier. In some instances it was possible to distinguish between species with overlapping mass spectra (e.g., between S_5 and Se_2, or between S_6 and SSe_2) by selecting mass peaks corresponding to a possible sum of the isotopic masses of one of the interfering species but not of the other.

Perhaps a better alternative assumption is that a long-chain phase exists at this composition and that the various Se_mS_n species observed in the vapor are degradation products of the long-chain polymer (and their electron-impact fragmentation products). This would seem to be more in harmony with the phase diagram of S–Se.[16]

4. Crystals from Sec. 3 Recrystallized over a Two-Month Period

The mass spectrum shows the same general form as was obtained with Crystal (3) and detailed previously in Table VI. The stepwise diminution appears smaller (about a factor of 2 between successive substitutions of seleniums), but this could be due to irreproducibility in the surface temperatures of the two samples. If the heats of sublimation of pure sulfur and pure selenium can be taken as a guide, the differences in volatility among the various substituted S–Se species within a group will become less significant as the surface temperature is increased.

The above results make the considerations of Zhuravlayeva and Chufarov[17] regarding separation of sulfur–selenium solutions by distillation appear rather naive.

The more recent investigations[3a–3d] appear to agree that significant concentrations of mixed sulfur–selenium molecules exist in both the condensed and vapor phases, but there appears to be a difference of opinion as to whether these mixed molecules are chain[3c] or ring[3d] structures.

In our earlier studies of vaporization of ring (orthorhombic sulfur monocrystals) and chain (S_μ) forms, it was possible to distinguish the two by their significantly different mass spectra. The two corresponding forms of selenium did not produce significantly different mass spectra, however. On this basis, it is difficult to decide from the data in Table VI whether the condensed phases involve rings or chains, but it is almost certain[1d] that the vapor species are rings.

I. Measurements of Appearance Potentials

Out of the large number of species observed, the only molecules chosen for appearance-potential measurements were those whose intensities were sufficient to permit of reasonable accuracy. Those investigated are listed in Table VII with measured values. The appearance potential of Se_2^+ was obtained during the CdSe experiments, when the thermodynamic evidence indicated that it was a parent. The method of extrapolated differences was used, with respect to both Cd^+ and residual Hg^+. The results agreed within 0.08 eV. The appearance potentials of the other selenium species were obtained above pure selenium. The Se_8^+ and Se_4^+ are presumably fragments under these conditions. The appearance potential of S_7Se^+ was measured with respect to S_8 during the studies on the mixed crystal grown from a melt.

IV. COMPUTATIONS

A. SrSe and $D_0(Se_2)$

From the experimentally measured atomic-selenium pressure of this system at 1853°K (Sec. III.A), the relative ion intensities of Se_2^+ and Se^+ (Table I), and the relative ionization cross sections of Se_2 and Se (Table II), one may directly calculate that the standard free-energy change for the reaction

$$Se_2(g) \rightarrow 2Se(g) \tag{9}$$

is $\Delta F°_{1853} = +27.70_6$ kcal/mole.

The free-energy function for Se_2 can be computed from the molecular parameters given by Herzberg,[18] with one important additional consideration. The magnetic-susceptibility results of Massen, Weijts, and Poulis[19] give strong evidence that the electronic ground state of Se_2 is $^3\Sigma$, and hence this has been assumed in the calculation of the free-energy function. The free-energy function of monatomic selenium has been taken from Stull and Sinke.[14] Thus, for Reaction (9) we obtain $\Delta H_{298} = 71.6 \pm 2$ kcal/mole and hence $D_0(Se_2) = 3.1 \pm 0.1$ eV.

Gaydon[20] has outlined the spectroscopic information as follows. (1) Transitions from a lower state ($^1\Sigma_g^+$, according to a rotational analysis[21]) to an upper state $[B(^1\Sigma_u^+)?]$ commence at 26 035 cm^{-1} (3.22 eV). The upper state converges rapidly; levels are known over

TABLE VII. Electron-impact appearance potentials of some selenium and sulfur–selenium molecules.

Ionic species	Appearance potential (eV)
Se_2^+	$9.2_3 \pm 0.1_5$
Se_3^+	$10.4_8 \pm 0.3$
Se_4^+	$10.1_3 \pm 0.3$
Se_5^+	$8.6_3 \pm 0.2$
Se_6^+	$8.8_8 \pm 0.2$
Se_7^+	$8.3_8 \pm 0.2$
Se_8^+	$8.6_3 \pm 0.2$
S_7Se^+	$9.3_5 \pm 0.2$[a]

[a] The measurement shows that the appearance potential of S_7Se^+ is 0.25 eV less than that of S_8^+. The S_7Se^+ value listed in the table was computed from the S_8^+ value given in Ref. 1(a).

---

[16] Max Hansen, *Constitution of Binary Alloys* (McGraw-Hill Book Co., Inc., New York, 1958), p. 1162.

[17] M. G. Zhurovleva and G. I. Chufarov, Zh. Prikl. Khim. **24**, 28 (1951).

[18] G. Herzberg, *Molecular Structure and Molecular Spectra. I. Spectra of Diatomic Molecules* (D. Van Nostrand Co., Princeton, N. J., 1950).

[19] C. H. Massen, A. G. L. Weijts, and J. A. Poulis, Trans. Faraday Soc. **60**, 317 (1964).

[20] A. G. Gaydon, *Dissociation Energies and Spectra of Diatomic Molecules* (Chapman and Hall, Ltd., London, 1953).

[21] E. Olsson, Z. Physik **90**, 138 (1934); dissertation, Stockholm, 1938; B. Rosen, Physica **6**, 205 (1939).

a range of 0.6 eV, and graphical extrapolation gives $D=0.75\pm0.1$ eV and thus a limit at $3.22+0.75=3.97\pm0.1$ eV. Predissociation is observed at 3.5 eV; consequently the above limit is for dissociation to excited products. If we accept all of the above, and furthermore assume with Gaydon that the upper state dissociates into $^3P+^1D$, then the limit for dissociation to normal products stands at 2.78 eV, which is the figure Gaydon recommends.

However, the rotational analysis requires a $^1\Sigma_g^+$ lower state, whereas magnetic-susceptibility measurements[18] indicate that a large fraction of the Se_2 must exist as $^3\Sigma$. All of the preceding information is in harmony with the current results if it is assumed that the $^1\Sigma_g^+$ lower state lies ~0.3 eV above a $^3\Sigma_g$ ground state. If the upper state B is indeed $^1\Sigma_u^+$, spectroscopic problems involving violation of the Wigner–Witmer correlation rules arise and require further elucidation.

Subsequent to the completion of this work, Barrow[22] has informed us of some extensive spectroscopic studies performed by him and his collaborators on Se_2. The aspects of his work that are most relevant to this discussion are the following. (a) His interpretation differs significantly from Olsson's[21] in that he finds the ground-state coupling to be shifted very far in the direction of Hund's Case (c). It is thus appropriate to use (approximately) an electronic multiplicity of 3 in computing the entropy of Se_2. The internuclear distances and vibrational frequency used in our computations are not affected greatly by this analysis. (b) From observed predissociations, Barrow and collaborators find $D_0(Se_2)=72.94\pm0.03$ kcal/mole, in excellent agreement with our less accurate figure.

The data presented in Table I enable one to estimate $D_0(SrSe)$ as well. Consider the gas-phase reaction

$$Se_2+Sr\rightarrow SrSe+Se, \qquad (10)$$

which is independent of pressure calibrations. The equilibrium constant may be computed in straightforward fashion allowing for isotopic abundances and the ionization cross sections given in Table II.[23] In this way, the equilibrium constant is found to be 0.325 and the standard free-energy change is $\Delta F°=+4.139$ kcal/mole. The free-energy functions of Se_2 and Se have already been discussed and that of Sr may be readily obtained.[14] We are left with the problem of estimating the free-energy function of SrSe. The internuclear distance is estimated (as was done in the analogous SrS[1c]) by reducing the sum of the crystal radii[24] by 20%. The vibrational force constant is then estimated by Badger's rule[25] to be 1.25×10^5 dyn/cm. The change in free-energy function (0°K) obtained from these considerations is +4.284 eu for Reaction (10), and correspondingly $\Delta E_0°=12.1$ kcal/mole. Taking the dissociation energy for Se_2 obtained in the present work, we conclude that $D_0(SrSe)=59.1\pm3$ kcal/mole$=2.5_7\pm0.1_5$ eV.

B. Absolute Equilibrium Constants and Free Energies of Formation of the Se_n Species

We have already determined the reaction enthalpies relating the various Se_n to one another. (Table V summarizes these results for all Se_n except Se_4 which could not be determined.) We now require only the free energies of formation to completely characterize the system thermodynamically. Their determination is, however, a formidable task. If the standard free energies of formation of the condensed phase CdSe or SrSe were well known, one could arrive at the corresponding $\Delta F_f°$ of Se_2(g) and Se(g). In the absence of reliable data of this type, more indirect methods are necessary. Several were tried and are detailed below.

(1) We assume that the ion intensities for Se_8^+, Se_7^+, Se_6^+, Se_5^+, and Se_2^+ in Table IV, Column 2, were all due to parent ions, and make corrections for isotopic abundance, secondary-electron yield, and (estimated) ionization cross sections.[26] These corrected ion ratios are then taken as the ratios of partial pressures of the Se_n. Making use of the vapor pressure of pure selenium given by Niwa and Shibata,[7] whose work covers this experimental range, it is possible to arrive at the partial pressure of each of these species, and hence to obtain absolute equilibrium constants. This approach is expected to be satisfactory for relating Se_8 and Se_7 (and possibly Se_5) to Se_6, but it runs into difficulty with Se_2 because of the uncertain fragmentation contribution. In the case described, Se_2 appears to constitute 20% of the saturated vapor at 469°K. That this is much too high can be shown by computing the heat of formation of Se_2 that corresponds to such a partial pressure, combining it with the heat of formation of Se_6(g) from Table V, and showing that the resulting enthalpy change for Reaction (6) is in wide disparity with the directly measured value (Table V) for Reaction (6). This is indeed a rather sensitive measure of Se_2 in the saturated vapor, since the thermochemical cycle just described involves three times the heat of formation of Se_2. On this basis, one may estimate that $\sim5\%$ of the saturated vapor at 469°K is Se_2. The best value obtained in this way is $\Delta H_f(Se_2)_{298°K}=34.2\pm0.8$ kcal/mole.

(2) A consistency condition can now be applied by tying the Se_2–Se_6 equilibrium constant from Method

---

[22] R. F. Barrow (private communication).

[23] The ionization cross section of SrSe has been approximated as the sum of Sr and Se contribution in this instance.

[24] L. Pauling, *The Nature of the Chemical Bond* (Cornell University Press, Ithaca, N.Y., 1960).

[25] R. M. Badger, J. Chem. Phys. 3, 710 (1935).

[26] The ratios of the ionization cross sections of Se_8, Se_7, and Se_5 relative to that of Se_6 were taken in proportion to the number of atoms in the molecule. For Se_2, a value $\sigma(Se_6)/\sigma(Se_2)=1.5$ was initially chosen, but the final selection of the partial pressure of Se_2 was based on subsequent considerations.

TABLE VIII. Partial pressure of Se_2 as a function of total selenium pressure at 500°C. All pressures are in atmospheres$\times 10^{-4}$.

Total selenium pressure	$P(Se_2)$ given by Brebrick,[a] if only the optical density at 3405 Å is used.	$P(Se_2)$ given by Brebrick,[b] using a correction to Column 2 obtained by measuring the absorption at 2100 Å	This work
1.18	0.8	0.5_5	0.80
2.50	1.5	0.8	1.17
3.55	2.0	0.9	1.36
4.34	2.4	1.0	1.48

[a] Reference 15.

[b] A reading error of a few percent has no doubt been incurred in abstracting Brebrick's data from his semilogarithmic curve.

(1), above, to another such constant obtained under those higher temperature conditions for which $Se_2^+ \gg Se_6^+$, and hence fragmentation is avoided. Some pressure calibration is needed in this instance. With two equilibrium constants measured at widely separated temperatures, one may once again calculate the enthalpy change for Reaction (6). By the use of the aforementioned 5% Se_2 in the saturated vapor, the ΔH does in fact agree fairly well with the directly measured ΔH for Reaction (6).

(3) One may of course, use the various experimental determinations of vapor density together with mass spectra to try to apportion the contributions of the various Se_n, but we prefer to use these for a final comparison with the data and inferences from this study.

(4) Brebrick[15] attempted to measure the partial pressure of Se_2 in selenium vapor by optical absorption. Within his wavelength range he found two regions, centered at 2100 and 3405 Å, where absorption was taking place due to Se_2 and a presumed Se_n species. By observing the variation of the optical density at both these wavelengths as a function of temperature and degree of undersaturation of selenium vapor, he deduced the contribution of Se_2 alone. He normalized his intensities by initially operating at such low vapor densities that Se_2 was the only significant contributor. The most sensitive test of his data is at a temperature of 500°C, since at lower temperatures his corrections are too uncertain, and at higher temperatures Se_2 comprises a larger fraction of the vapor and hence variations are not as noticeable. In Table VIII, two sets of data have been abstracted from Brebrick's graph, and compared with the present results. One involves the optical absorption at 3405 Å only; the other uses the absorption at 2100 Å to take into account the absorption due to other species. The current results fall between these two sets.

TABLE IX. Partial pressures of Se_n species in saturated Se vapor at $T=469$°K.

Molecular species	Pressure (atm)
Se_2	6.04×10^{-8}
Se_5	3.30×10^{-7}
Se_6	4.84×10^{-7}
Se_7	1.28×10^{-7}
Se_8	1.9×10^{-8}

TABLE X. Variation of the equilibrium constant with temperature for various selenium reactions. The constants given below assume the simple function $\log K_P = (A/T)+B$ in each case.

Reaction	A	B
$2\ Se_3 \rightarrow 3\ Se_2$	−5 625	$+8.17_7$
$Se_6 \rightarrow 3\ Se_2$	−14 200	$+14.9_6$
$5\ Se_6 \rightarrow 6\ Se_5$	−12 100	$+18.4_4$
$6\ Se_7 \rightarrow 7\ Se_6$	−3 090	+3.74
$3\ Se_8 \rightarrow 4\ Se_6$	−3 600	+5.60
6 Se (solid)$\rightarrow Se_6$	−7 370	+9.40
6 Se (liquid)$\rightarrow Se_6$	−4 360	+3.30

Table IX summarizes the deduced partial pressures for saturated selenium vapor at 469°K.

The free energy of formation of $Se_3(g)$ can be calculated by use of Reaction (7) and the data in Table III, together with the vapor pressure of CdSe.[9,11] In this way, one arrives at an equilibrium constant of 241 for Reaction (7) at 971°K. The best that can be done for Se_4 is to place a limit on its stability by making use of the data in Table III.

By utilizing the results of this section, together with the previously deduced enthalpies, one can derive a temperature variation for each of the reactions listed in Table V. This has been done in Table X, in the functional form $\log K_p = A/T+B$, where all partial pressures are in atmospheres, and the temperature is in degrees Kelvin.

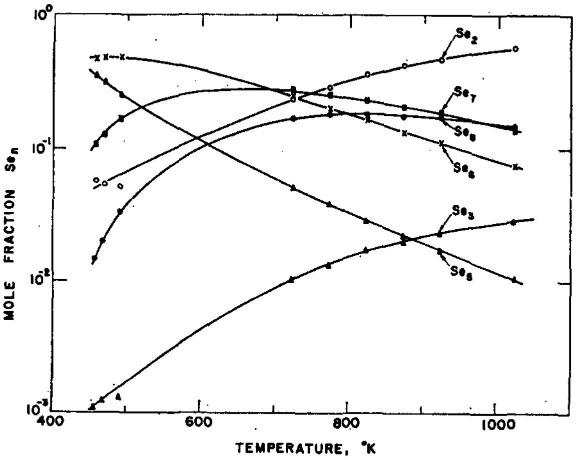

FIG. 9. Composition of saturated selenium vapor derived from equilibrium-constant measurements.

TABLE XI. Comparison between the values of the mean number ν of Se atoms per molecule as obtained from vapor-density measurements and the values calculated from the equilibrium constants obtained in the present study.

Temperature (°K)	Pressure (mm Hg)	ν		Experimental reference
		Calculated	Experimental	
469	9.18×10^{-4}	5.64	5.286 5.419	7(c)
480	2.07×10^{-3}	5.70	5.278 5.412	7(c)
480.9		5.71	5.90	7(b)
502	8.63×10^{-3}	5.81	5.230 5.372	7(c)
513	1.53×10^{-2}	5.84	5.205 5.351	7(c)
524	2.65×10^{-2}	5.87	5.181 5.331	7(c)
535	4.52×10^{-3}	5.89	5.159 5.312	7(c)
723	7.0	4.66	4.84	7(a)
773	9	3.41	3.88	7(a)
	27	4.89	4.46	
	34	5.16	4.84	
823	11	2.35	3.33	7(a)
	41.5	3.86	3.93	
	89	4.92	4.90	
823	26.5	3.23	3.617	7(d)
	41.6	3.87	4.125	
	62.8	4.46	4.506	
873	14.5	2.08	2.70	7(a)
	68	3.05	3.30	
	186.5	4.52	4.45	
873	34.7	2.38	2.903	7(d)
	85.7	3.36	3.751	
	170.2	4.38	4.414	
923	18	2.03	2.28	7(a)
	106	2.51	2.90	
	460	4.51	4.32	
923	44.9	2.11	2.349	7(d)
	142.4	2.81	3.260	
	298.2	3.85	4.113	
973	20.5	2.06	2.13	7(a)
	107	2.30	2.33	
	248	2.65	2.87	
	562	3.34	3.72	
973	52.4	2.14	2.103	7(d)
	138.3	2.37	2.529	
	216.5	2.57	2.837	
	369.3	2.94	3.345	
1023	22.5	2.01	2.04	7(a)
	104	2.03	2.09	
	222	2.10	2.40	
	343	2.22	2.60	
	517	2.47	2.90	
	710	2.79	3.16	
1023	89.9	2.03	2.069	7(d)
	163.0	2.06	2.227	
	465.0	2.39	2.846	
1073	860	2.34	2.66	7(a)
1173	1126	2.06	2.19	7(a)

C. Calculation of ν, the Mean Number of Selenium Atoms per Molecule

From the considerations of the previous section, we can relate each of the Se_n species (except Se_4) to one, say Se_6. Thus, for a particular experimental temperature and selenium pressure, it is possible to compute the contribution of each of the Se_n to the vapor composition. It is of particular interest to choose those temperatures and pressures that correspond to the conditions of the various vapor-density experiments.[7] The actual computations are quite tedious, involving the solution of an eighth-degree equation, and have been performed with the aid of an IBM-7094 computer. The detailed composition of the vapor at each experimental condition has been converted into an average number of atoms per molecule. In Table XI, the results are compared with the results of the various experimenters. The calculated values lie somewhat higher than the experimental vapor-density results at the low temperatures, and consistently lower than the experimental densities at the higher temperatures. This trend suggests that a slight increase in the ΔH of Reaction (6) might improve the high-temperature fit. This adjustment is rather sensitive; merely doubling the ratio of Se_2 to Se_6 at 823°K overcompensates for the deviation from the vapor-density measurements, but it only reduces the ΔH of Reaction (6) to 63.5 kcal/mole. In view of the approximations involved in excluding specific-heat corrections and nonideality of the vapor, it is probably not meaningful to attempt a much better adjustment.

D. Composition of the Saturated Vapor

From the vapor pressure of selenium[7,27] at various temperatures and the calculated equilibrium constants, we may compute a saturated vapor composition over the accessible ranges of temperature and pressure.

---

[27] L. S. Brooks, J. Am. Chem. Soc. 74, 227 (1952).

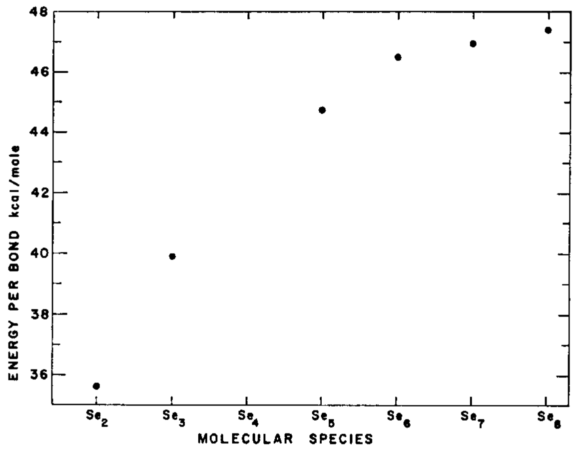

FIG. 10. Energy per bond of selenium rings as a function of the size of the ring.

The results of such a calculation are shown in Fig. 9. The contrast with a corresponding curve[1a,1d] for S_8 is noteworthy. At the lowest temperatures, sulfur vapor is dominated by the contributions of S_8 (and to a lesser extent S_6 and S_7). This predominance of the larger rings continues right up to the boiling point. In selenium vapor, the lowest temperature measurements show a dominance by Se_6 and Se_5 (and 10% Se_7), but at the boiling point Se_2 is the most important species.

It should be borne in mind that the limit placed on Se_4 is not low enough to permit neglect of its influence in the vapor. The one measurement recorded in Table III would imply that Se_4 constitutes ~25% of the saturated vapor at 971°K. This is, of course, an upper limit to the Se_4 contribution.

E. Energy Per Bond in the Selenium Rings

From the data in Table V and the calculated value of $D_0(Se_2)$, one may readily deduce the heats of atomization of each of the selenium species. If each species is assumed to be a ring and the total heats of atomization are divided by the number of bonds per ring, the curve shown in Fig. 10 results. It is to be noted that, if stability is defined as atomization energy per bond, then Se_8 is more stable than Se_6 although Se_6 is much more abundant in selenium vapor. The sulfur system displays a similar curve,[1a] although in that case S_8 is the most abundant molecular species in the saturated vapor over the commonly measured range. It is obvious from this comparison that the abundance of S_8 in sulfur vapor is not just a consequence of its greater energy per bond; it is also an accident of the volatility of sulfur. The selenium bonds are, on the average, ~0.5 eV weaker than the corresponding sulfur bonds.

V. CONCLUSIONS

(1) The dissociation energies of Se_2 and SrSe are found to be 71.2 ± 2 and 59.1 ± 3 kcal/mole, respectively, at 0°K.

(2) The heats of formation of Se_n are 34.2 ± 0.8 kcal/mole for Se_2, 38.4 ± 1.5 kcal/mole for Se_3, 40.5 ± 1.5 kcal/mole for Se_5, 37.6 ± 1.5 kcal/mole for Se_6, 41.5 ± 1.5 kcal/mole for Se_7, and 44.5 ± 1.5 kcal/mole for Se_8. No temperature dependence and hence no heat of formation could be measured for Se_4 because of its weak intensity.

(3) The detailed molecular composition of selenium deduced from the current mass-spectrometric study is in reasonable agreement with several vapor-density measurements.

(4) A plot of the energy per bond vs size of the ring shows a maximum or plateau at the Se_8 position.

(5) No obvious nonequilibrium vaporization (of the type observed with sulfur) takes place with selenium.

(6) Sulfur–selenium mixed molecules do not form easily at room temperature. They do readily form at higher temperatures (~300°C) and upon cooling they remain "frozen in," and can then be observed readily in the vapor.

(7) The heat of fusion of selenium is found to be 2.30 kcal/mole.